



Quantifying soil carbon loss and uncertainty from a peatland wildfire using multi-temporal LiDAR



A.D. Reddy^{a,*}, T.J. Hawbaker^b, F. Wurster^c, Z. Zhu^a, S. Ward^d, D. Newcomb^d, R. Murray^c

^a U.S. Geological Survey, Reston, VA, U.S.A.

^b U.S. Geological Survey, Denver, CO, U.S.A.

^c U.S. Fish and Wildlife Service, Suffolk, VA, U.S.A.

^d U.S. Fish and Wildlife Service, Raleigh, NC, U.S.A.

ARTICLE INFO

Article history:

Received 30 September 2014

Received in revised form 17 August 2015

Accepted 23 September 2015

Available online 9 October 2015

Keywords:

Soil carbon

Fire

Peatlands

LiDAR

Vertical accuracy

ABSTRACT

Peatlands are a major reservoir of global soil carbon, yet account for just 3% of global land cover. Human impacts like draining can hinder the ability of peatlands to sequester carbon and expose their soils to fire under dry conditions. Estimating soil carbon loss from peat fires can be challenging due to uncertainty about pre-fire surface elevations. This study uses multi-temporal LiDAR to obtain pre- and post-fire elevations and estimate soil carbon loss caused by the 2011 Lateral West fire in the Great Dismal Swamp National Wildlife Refuge, VA, USA. We also determine how LiDAR elevation error affects uncertainty in our carbon loss estimate by randomly perturbing the LiDAR point elevations and recalculating elevation change and carbon loss, iterating this process 1000 times. We calculated a total loss using LiDAR of 1.10 Tg C across the 25 km² burned area. The fire burned an average of 47 cm deep, equivalent to 44 kg C/m², a value larger than the 1997 Indonesian peat fires (29 kg C/m²). Carbon loss via the First-Order Fire Effects Model (FOFEM) was estimated to be 0.06 Tg C. Propagating the LiDAR elevation error to the carbon loss estimates, we calculated a standard deviation of 0.00009 Tg C, equivalent to 0.008% of total carbon loss. We conclude that LiDAR elevation error is not a significant contributor to uncertainty in soil carbon loss under severe fire conditions with substantial peat consumption. However, uncertainties may be more substantial when soil elevation loss is of a similar or smaller magnitude than the reported LiDAR error.

Published by Elsevier Inc. This is an open access article under the CC BY-NC-ND license (<http://creativecommons.org/licenses/by-nc-nd/4.0/>).

Contents

1.	Introduction	307
2.	Methods	307
2.1.	Study area	307
2.2.	Lateral west fire	309
2.3.	LiDAR data collection	309
2.4.	Soil data	309
2.5.	Measured estimation of soil carbon loss and uncertainty	309
2.6.	Modeled estimation of soil carbon loss	309
3.	Results	310
3.1.	Soil sampling	310
3.2.	Elevation change from LiDAR	310
3.3.	Uncertainty in elevation change from LiDAR	310
3.4.	Soil carbon loss and uncertainty from LiDAR	311
3.5.	Soil carbon loss from FOFEM (model)	311
4.	Discussion	311
4.1.	Comparison of carbon estimation methods: model vs. LiDAR	311
4.2.	Multi-temporal LiDAR for soil carbon loss estimation	311
4.3.	Comparison to other studies of fire carbon emissions	313
4.4.	LiDAR vertical accuracy error	314

* Corresponding author.

5. Conclusion	315
Acknowledgments	315
References	315

1. Introduction

Peatlands account for 3% of global land cover, yet are a major reservoir of global soil carbon, accounting for 270–1672 Pg C in the upper northern latitudes alone (Gorham, 1991; Tarnocai et al., 2009; Turunen, Tomppo, Tolonen, & Reinikainen, 2002; Yu, Loisel, Brosseau, Beilman, & Hunt, 2010). In many peatland environments, high water tables limit the decomposition rate of dead plant material and contribute to an accumulation of carbon-rich organic soil (Clymo, 1984). Over thousands of years, peatlands in places like tropical Indonesia or boreal Russia can develop peat soil profiles several meters in depth. As a result, researchers have come to view these unique ecosystems as important stores of terrestrial carbon (Page, Rieley, & Banks, 2011).

In the United States, peatlands are found in Alaska, Midwestern States such as Minnesota, and the coastal plain of Virginia and North Carolina (Mitsch, Gosselink, Anderson, & Zhang, 2009). Over the past few centuries, U.S. peatlands have been subjected to peat harvesting, converted to agriculture, or logged, activities that have threatened their ability to serve as carbon sinks (Lily, 1981; Richardson, 1983). In addition, the intentional draining of these water-logged ecosystems has significantly altered their hydrology and may be contributing to an increase in the frequency and severity of wildfires in the United States and abroad (Frost, 1989, 1995; Turetsky, Donahue, & Benschoter, 2011).

Peat soils are carbon rich and because combustion can occur in spite of high fuel moisture levels (Reardon, Curcio, & Bartlette, 2009), fires in peatland ecosystems can persist for several months and burn to depths greater than one meter below the surface, emitting terrestrially sequestered carbon to the atmosphere and contributing to global greenhouse gas emissions. Quantifying this carbon loss is necessary for understanding the peatland carbon cycle and for determining whether policies aimed at preserving and restoring peatlands may also help offset fossil fuel emissions and mitigate climate change.

Several studies have estimated soil carbon loss resulting from peat fires. One set of approaches has been to simulate a fire's effects (French et al., 2011). Models like the First-Order Fire Effects Model (FOFEM) use information about fuel availability, moisture content, and season to estimate tree mortality, fuel consumption, and greenhouse gas emissions (Reinhardt, Keane, & Brown, 1997). This approach is limited because assumptions about the maximum duff depth and the spatial heterogeneity of the peat depth may limit the model's ability to characterize the effects of a severe fire.

An alternative approach to carbon loss modeling has been to measure the total soil volume consumed in the fire, and then multiply this value by the burned soil's bulk density and carbon content. The volume can be estimated from elevation measurements of the soil surface from before and after the fire. Light detection and ranging (LiDAR) instruments are often the source of this elevation data. Discrete-return LiDAR measures the elevation of a land surface at fine spatial resolutions by recording the time delay in a high-frequency laser pulse that travels from the sensor to a target and back. Each laser pulse may have one or more returns representing different physical objects and their elevations. The last returns to be recorded by the sensor are generally the lowest physical objects on the Earth's surface and are often indicative of the soil surface itself.

While LiDAR data are often used for post-fire elevation, pre-fire data are seldom available. As a result, studies typically either assume an average burn depth or use elevations of unburned areas as analogs for the pre-fire surface (Ballhorn, Siegert, Mason, & Limin, 2009; Page et al., 2002; Poulter, Christensen, & Halpin, 2006). These approaches

may not accurately represent pre-fire elevations and thus an approach that uses spatially detailed height data from before and after a disturbance is needed. Our study is the first, to the best of our knowledge, to overcome this obstacle by using both pre- and post-fire LiDAR elevation data to characterize the elevation change and total soil carbon loss resulting from a temperate peatland fire. Doing so eliminates most of the uncertainty from having to estimate pre-fire elevation through other methods.

A second aim of this study is to determine how LiDAR vertical accuracy error contributes to uncertainty in estimates of soil carbon loss from fire. The vertical error of an elevation dataset is typically quantified as the root mean squared error (RMSE), and frequently ranges from 5 to 20 cm. The discrepancy between a LiDAR-derived elevation and an estimate from a more accurate method, such as ground-surveying, may be caused by errors inherent to the components of the LiDAR sensor, such as the global positioning system, inertial mass unit, and laser. Error in elevation measurements can also vary by land cover and surface slope (Hodgson & Bresnahan, 2004). In addition, incorrect classification of LiDAR points, such as when a ground return is actually low-lying vegetation, may contribute to vertical error.

Because error is inherent to LiDAR collection and use, there is a need to understand how it might affect the accuracy of derived products, such as estimates of peatland elevation and carbon loss. Quantifying how elevation error might affect LiDAR-derived estimates like carbon loss is important for judging the accuracy of the pre- and post-fire estimation method.

This work ultimately addresses two main research questions. First, how much soil carbon was consumed by the 2011 temperate peat fire in Great Dismal Swamp National Wildlife Refuge, USA? In answering this question, we make use of both pre- and post-fire LiDAR elevation data. We also compare the LiDAR-based results to modeled estimates from FOFEM to determine the utility of fire emissions models in the context of peatlands. The second question we attempt to answer is to what extent the LiDAR vertical accuracy error affects the soil carbon estimate. If the error is considerable, then LiDAR-based methods of estimating elevation change and soil carbon loss in peatlands may not be preferable to other techniques, such as modeling.

2. Methods

2.1. Study area

The 45,000 ha Great Dismal Swamp National Wildlife Refuge (GDSNWR) is a forested wetlands ecosystem located on either side of the North Carolina–Virginia, USA border and situated within 20 miles of the Atlantic Ocean, Chesapeake Bay and Albemarle Sound (Fig. 1). Its climate is characterized by warm, humid summers and mild winters. Monthly mean temperatures between 2005 and 2014 ranged from 11.7° Celsius in January to 32.9 °C in July (53.0 to 79.6° Fahrenheit) at a weather station on the Eastern edge of the refuge. Precipitation is distributed throughout the year with slightly greater rainfall in the summer months. Mean annual rainfall over the last decade was 1413 mm, and ranged from 996 mm in the driest year to 1820 mm in the wettest (Peterson & Vose, 1997).

The refuge has low relief, with a surface elevation around 7 m above sea level along the western edge that declines to between 4 and 5 m to the east and southeast. Two- to three-meter peat deposits overlie clay soils throughout the swamp. The refuge is seasonally flooded, and is characterized by the presence of water at or near the soil surface during

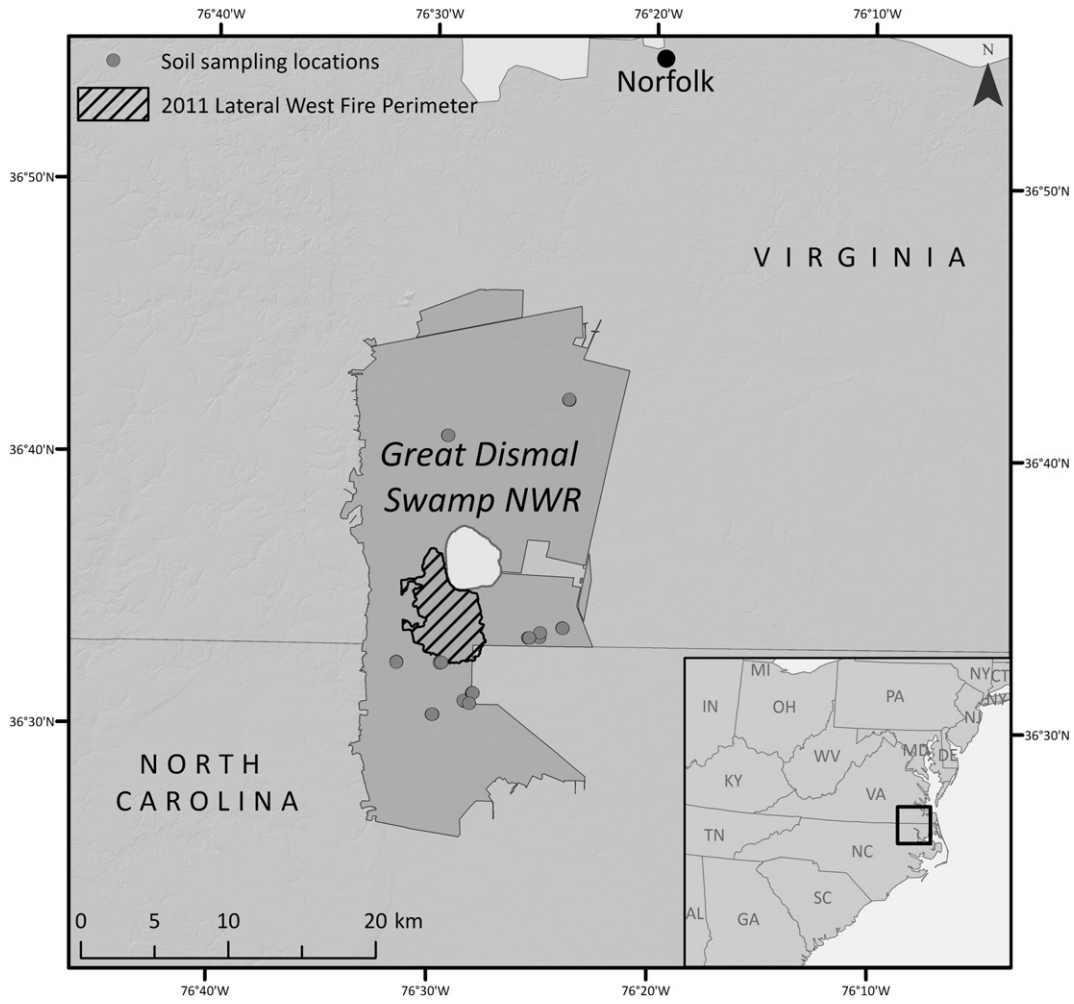


Fig. 1. Map of Great Dismal Swamp NWR. The hatched area shows the perimeter of the Lateral West fire; the white polygon to the northeast is Lake Drummond.



Fig. 2. The image to the left is an aerial view of the Lateral West fire taken a few weeks following ignition in August 2011. Top-right, a tree stump and roots are exposed by the fire. Bottom-right, vegetative regrowth is apparent in waterlogged conditions by 2013. Credits: Mark Jamieson/USFWS (left), Steve Bingham/USFWS (top-right), Ashwan Reddy (bottom-right).

the winter and spring. During summer, vegetative growth draws the water down and leads to dry conditions by autumn.

A 158-mile network of roads and drainage ditches traverses the landscape, built by logging companies and other commercial interests before the refuge's formation in 1974. The ditches were intended to drain the underlying soils and facilitate timber harvesting. Construction of the ditch network in GDSNWR is thought to have created progressively drier conditions throughout the swamp and increased the risk of fire (Day, 1982; Levy, 1991). Studies of artificially drained peatlands have found that peat oxidation, subsidence and changes in the plant community are common (Mälson, Backéus, & Rydin, 2007; Pronger, Schipper, Hill, Campbell, & McLeod, 2014; Talbot, Richard, Roulet, & Booth, 2010).

2.2. Lateral west fire

On August 4, 2011, lightning ignited a fire within the refuge that burned for 126 days. Dubbed the Lateral West fire, this disturbance affected 25 km² of the refuge and overlapped with the burn scar from the South One fire in 2008. A combination of limited rainfall and human-altered hydrology likely exacerbated the conditions leading to the Lateral West fire. In the aftermath, few trees were left standing and soil loss of more than one meter was observed in some areas. Fig. 2 shows an aerial view of the fire scar a few weeks following ignition. The dense stand of trees in the foreground gives way to a landscape opened up by a combination of the 2008 South One and 2011 Lateral West fires. Smoke is apparent despite the foot of water that Hurricane Irene left in the days preceding the photo. Fig. 2 (top-right) depicts a tree stump whose roots have been exposed by the severe fire. By 2013 (Fig. 2; bottom-right), two years post-fire, many areas are waterlogged, providing an opportunity for emergent vegetation to take hold. The relatively severe fire and data availability made the 2011 Lateral West fire at Great Dismal Swamp an ideal case study for determining carbon loss and understanding the effect of LiDAR error on this estimate.

To assess the soil carbon loss, the study was limited to the fire's perimeter (Fig. 1). This extent was delineated using GPS while flying the fire boundaries of the burn scar at low altitude in a helicopter; the vegetation in GDSNWR is extremely dense and ground travel and surveys are extremely difficult. The GPS data were converted to a polygon shapefile and loaded into a GIS for analysis with elevation and soil information.

2.3. LiDAR data collection

Pre-fire LiDAR data were collected in March 2010 using a LH Systems ALS50 LiDAR system at a flying height of 2138 m above sea level. The U.S. Geological Survey (USGS) maximum nominal post spacing requirement of 0.7 m was met by the flight. Points were classified as ground or non-ground using TerraScan software (Terrasolid, 2005). The root mean square error of the ground points was determined to be 9 cm, based on comparisons with 35 control points. Post-fire LiDAR data were obtained in August 2012 using a Leica ALS70 500 kHz Multiple Pulses in Air (MPiA) LiDAR sensor system at a flying height of 2382 m above sea level. Flight lines had a 29.9% overlap and the nominal post spacing was <0.7 m. LiDAR data were classified as ground and non-ground points using TerraScan software. A 7 cm root mean square vertical error was calculated for the ground points based on comparison with 8 control points. While additional ground control points would have provided a better sense of the 2012 LiDAR vertical error, data collected by the LiDAR vendor were limited.

2.4. Soil data

Post-fire soil samples were collected from 23 unburned sites surrounding the fire perimeter during August 2013. The sampling locations were dispersed throughout the refuge and are depicted in Fig. 1.

Peat from these locations tends to be highly decomposed organic matter and is typically classified as Oa using the U.S. Department of Agriculture's Natural Resource Conservation Service's (NRCS) soil survey classification system (Schoeneberger, Wysocki, Benham, & Broderson, 2002). A standard core was used to obtain a sample volume of peat from each site to calculate bulk density. Samples were also processed using a combustion analyzer to determine total organic carbon and mineral content. Organic matter was calculated by subtracting mineral content from 100. All peat samples were sent to the NRCS Soil Survey Lab in Lincoln, NE, for analysis. Three additional samples were gathered from a 1999 biogeochemistry study of Atlantic White Cedar stands (Thompson, Belcher, & Atkinson, 2000). These were included because they represented a forest type that historically composed a sizable portion of GDSNWR. Resulting bulk densities and carbon values were averaged and used to calculate total carbon loss from the 2011 Lateral West fire.

2.5. Measured estimation of soil carbon loss and uncertainty

Fig. 3 provides a graphical summary of the workflow used to calculate total soil carbon loss and uncertainty from LiDAR vertical accuracy error. We divided the study area into 10-m grid cells. A finer resolution grid would have resulted in many cells that contained few to no LiDAR ground returns, while a larger resolution would have limited the spatial detail of the data. Although LiDAR data were obtained at high resolutions, the presence of dense vegetation and surface water led to just 1–2% of 2012 LiDAR returns being classified as ground.

We used a Monte-Carlo approach to better understand how the vertical error of individual points propagates to introduce uncertainty into the elevation, elevation change and carbon loss estimates. Within each grid cell, 1000 elevations were simulated for each LiDAR return by perturbing ground points within their known root mean squared errors, 9 and 7 cm for the 2010 and 2012 LiDAR datasets, respectively. As an example, Point 1 in Fig. 3A has a 2010 elevation of 500 cm (5 m). To simulate the point's uncertainty, a normal distribution of elevation with mean of 500 cm and standard deviation of 9 cm was created, from which 1000 elevations were randomly extracted. In Fig. 3B, 1000 simulated elevations have been created for each LiDAR return.

The elevations of the perturbed ground points were then averaged within 10 m grid cells to create a digital elevation model for each of the Monte-Carlo iterations (DEM; Fig. 3C). This step ultimately produced 1000 pre- and post-fire DEMs. Together the simulated DEMs represent the range of uncertainty resulting from the 2010 and 2012 LiDAR vertical RMSEs. Elevation change data were calculated by subtracting each set of pre- and post-fire DEMs from one another (Fig. 3D). For each of the 1000 resulting elevation change datasets, total carbon loss was then calculated by multiplying the cells with elevation loss by average soil bulk density and total organic carbon content, and aggregating the results within the Lateral West fire perimeter (Fig. 3E–F).

Ultimately, 1000 estimates of total carbon loss from the 2011 fire were produced that incorporated LiDAR error. We report mean elevation change and soil carbon loss within the fire perimeter and in the 500-m buffer surrounding the perimeter (across all 1000 iterations; Fig. 3G). We also provide these values for a 500-m buffer surrounding the fire to demonstrate elevation change and carbon loss in an unburned control area. Finally, carbon loss error due to LiDAR accuracy RMSE is reported based on the standard deviation of the carbon loss estimates.

2.6. Modeled estimation of soil carbon loss

In addition to the pre- and post-fire LiDAR analysis, we used the First-Order Fire Effects Model version 6.0 (FOFEM) to estimate greenhouse gas emissions from the 2011 Lateral West fire. For inputs, the Monitoring Trends in Burn Severity thematic burn severity raster layer was used to delineate the area burned (MTBS; Eidenshink et al.,

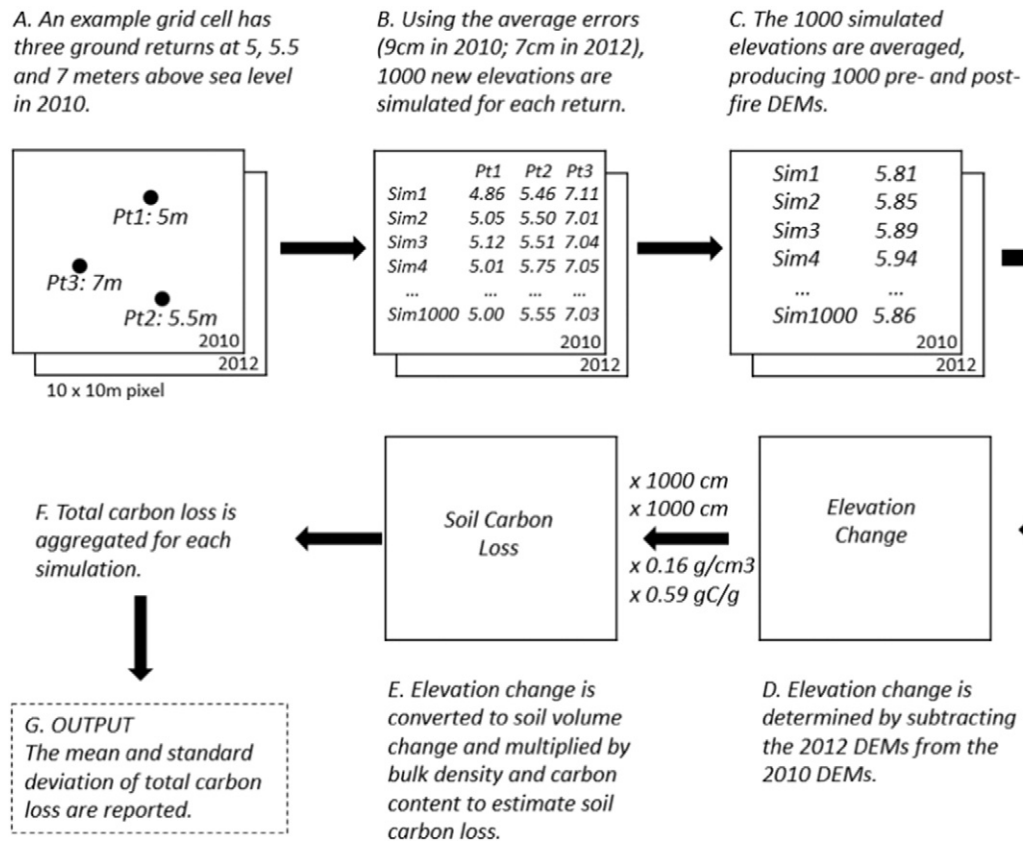


Fig. 3. LiDAR workflow to estimate carbon loss and uncertainty.

2007). This layer was combined with the LANDFIRE Fuel Loading Model raster layer (FLM; Lutes, Keane, & Caratti, 2009); we used version 1.1.0, which includes changes in fuel loads resulting from the South One fire in 2008. The FLM data are categorical and provide duff, litter, fine woody debris, and coarse wood debris loadings that can be used with FOFEM to estimate fuel consumption and greenhouse gas emissions.

In addition to fuel loads, FOFEM requires information about fuel moisture regime, percent of crown burned, region, cover group, and season. We set fuel moisture levels according to the MTBS severity class and guidance in the FOFEM version 6.0 User's Guide (Lutes, 2012), where unburned to very low severity pixels were assigned to a wet moisture regime, low severity pixels were assigned a moderate moisture regime, and moderate severity pixels were assigned a dry moisture regime. We also varied percent of the crown burned by the MTBS severity class, using 40%, 60%, and 80% for the unburned to very low, low, and moderate severity classes, respectively, following values used by Hawbaker and Zhu (2012). Region, cover group, and season were set to southeast, pocosin, and summer, respectively. Greenhouse gas emissions (CH_4 , CO , and CO_2) were estimated using FOFEM for each combination of FLM and MTBS severity class on a per unit basis and then converted to total carbon equivalents. Carbon emissions for each FLM and MTBS combination were then multiplied by the total area burned of each combination and summed across the entire area burned by the Lateral West fire for comparison with the pre- and post-fire LiDAR estimates of carbon loss.

3. Results

3.1. Soil sampling

Sixty-one soil samples were analyzed for bulk density and 44 samples examined for total organic carbon content. Bulk density within these histosol soil types ranged from 0.09 to 0.24 g/cm^3 and had a

mean of 0.16 g/cm^3 . Batjes (1996) demonstrates that peat soils vary in density from 0.03 to 0.94 g/cm^3 , with a mean of 0.31 g/cm^3 and a high coefficient of variation relative to other soil types. Our recorded densities were also similar to those of drained peat soils (Minkkinen & Laine, 1998). Total organic carbon accounted for between 46 and 64% of total soil matter among the 44 samples, with a mean of 59%. Consistent with the characteristics of peatland soils, organic matter averaged 95% among all samples. Mean values for bulk density and carbon content were used to convert elevation change to carbon loss.

3.2. Elevation change from LiDAR

The highest elevations within the fire perimeter in 2010 were about 6.5 m above sea level and tapered off to the east and northeast along Lake Drummond (Fig. 4, left). Fig. 4 (middle) illustrates that by 2012 the peat surface was lowered significantly. The average pixel-level elevation loss within the fire perimeter, calculated as the 2012 elevation minus the 2010 elevation, was 46 ± 18 cm (Table 1). The standard deviation here reflects the variability in average elevation change among pixels in the study area. The 500 m buffer area surrounding the burn scar experienced a mean elevation loss of 6 ± 37 cm. As depicted by the map in Fig. 4 (right), drops in elevation varied spatially and exceeded one meter in the southernmost portions of the fire.

3.3. Uncertainty in elevation change from LiDAR

One thousand Monte Carlo simulations of elevation change were produced for each pixel as part of our effort to understand the effect of LiDAR vertical accuracy error. We then determined the percent of those 1000 elevation change values that were less than 0 and thus represented a decline in ground elevation. The more values below zero, the more confidence we could have that a pixel actually decreased in elevation. Fig. 5 depicts the elevation change map between 2010 and 2012,

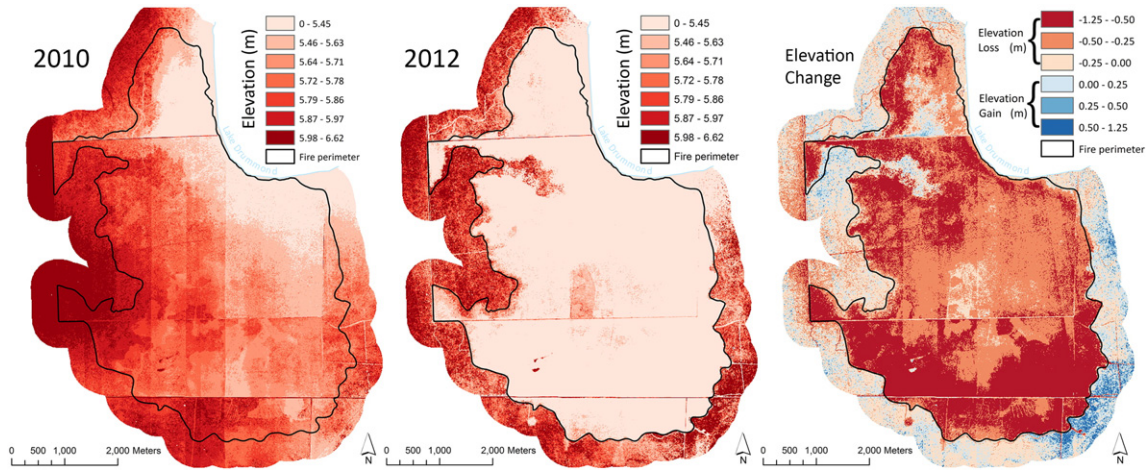


Fig. 4. Depicted are the 2010 (left) and 2012 (middle) LiDAR-derived surface elevations for the Lateral West fire scar and a 500 m buffer surrounding it. To the right, a map of elevation change calculated as the 2012 minus 2010 DEM is shown.

with pixels colored black to represent uncertainty about whether those areas underwent a positive or negative change in ground elevation. The three subsetted areas to the right in Fig. 5 depict levels of certainty about whether an elevation loss or gain occurred. We find that 0.16, 0.63, and 0.89% of all pixels within the fire perimeter did not meet the 67, 95 and 99% confidence levels, respectively. For these pixels, the median elevation change among the three confidence levels varied between -0.1 and -0.5 cm, values much smaller than the 9 and 7 cm root mean squared errors of the 2010 and 2012 LiDAR datasets. Removing the pixels that did not meet the 95% confidence level, we recalculated average elevation loss within the fire scar to be 47 cm.

3.4. Soil carbon loss and uncertainty from LiDAR

Given the opportunity for misclassifying elevation loss as gain and vice versa based on the influence of LiDAR error, we removed pixels that did not meet the 95% confidence level from the estimate of carbon loss. Based on the remaining pixels, total carbon loss was estimated to be 1.10 Tg C. The standard deviation around this estimate based on LiDAR vertical error was 0.00009 Tg C, which is 0.008% of total carbon loss.

While some areas within the burn perimeter experienced little to no change in soil carbon, the pixel-level average carbon loss per unit-area was found to be 44.3 kg C/m². Carbon loss was directly related to elevation loss, since mean bulk density and total organic carbon content values were applied to all areas. Fig. 6 provides spatial detail of carbon loss across the fire perimeter.

3.5. Soil carbon loss from FOFEM (model)

As a comparison to the LiDAR-based method, fire emissions were also estimated using the LANDFIRE Fuel Loading Model and Monitoring Trends in Burn Severity data as inputs to FOFEM. Carbon loss from

FOFEM varied according to the FLM type and MTBS severity class (Table 2). The burn scar area comprises four FLM types, each varying in amounts of duff, litter, fine woody debris (FWD) and large woody debris. According to the MTBS data of the Lateral West fire, 11% of the burned area was classified in the unburned to very-low severity class, 54% was in the low severity class, and 36% was in the moderate severity class.

Total carbon loss for the Lateral West fire estimated using FOFEM was 0.058 Tg C, much less than the 1.1 Tg C loss estimated using LiDAR. Average emissions per unit-area from FOFEM were 0.92 kg C/m². Carbon emissions increased with burn severity class (Table 2). FLM 101, which had the largest peat depth available to be burned (25 cm), produced the highest modeled emissions.

4. Discussion

4.1. Comparison of carbon estimation methods: model vs. LiDAR

The model approach using FOFEM estimated soil carbon loss at 0.06 Tg C across the entire 25 km² fire scar, a value considerably lower than the LiDAR-based 1.10 Tg C total. This discrepancy in estimates is due, in part, to the limitations of the fuel loading models that provide information on fuel availability to FOFEM. For this study region, the FLMs have shallow duff (peat) depths. FLM 101, which accounted for 22% of the burned area, had the largest maximum peat depth at 25 cm, nearly half the LiDAR-estimated 46 cm average decline in soil elevation. These shallow FLM peat depths limited the severity of the soil combustion in FOFEM and made it difficult to fully characterize the below-ground carbon loss.

Given the limitation of FLMs in the context of Great Dismal Swamp, the LiDAR-based method likely provides the best carbon estimation of temperate peat loss from fire. Other methods for determining soil elevation change exist, but they can be context-dependent. Mack et al. (2011), for instance, studied a peat fire in Alaska by deriving elevation change via sedges that survived the disturbance and could be used as pre-fire elevation markers. For most other environments though, tools like LiDAR are necessary to estimate elevation change.

4.2. Multi-temporal LiDAR for soil carbon loss estimation

Following the 2011 Lateral West fire at Great Dismal Swamp, we estimated soil carbon emissions using two methods. The remote sensing-based method using pre- and post-fire LiDAR data to assess spatially explicit soil elevation change and carbon loss resulted in a 1.10 Tg C estimate corresponding to an average 46 cm elevation loss. In the 500 m

Table 1
Mean and standard deviation of elevation and elevation change inside and outside the lateral west fire scar.

Area	Mean elevation (sd)
2010 fire scar	5.68 (0.20)
2010 500-m buffer	5.79 (0.58)
2012 fire scar	5.21 (0.23)
2012 500-m buffer	5.73 (0.64)
Area	Mean elevation change (sd)
Fire scar	-0.46 (0.18)
500-m buffer	-0.06 (0.37)

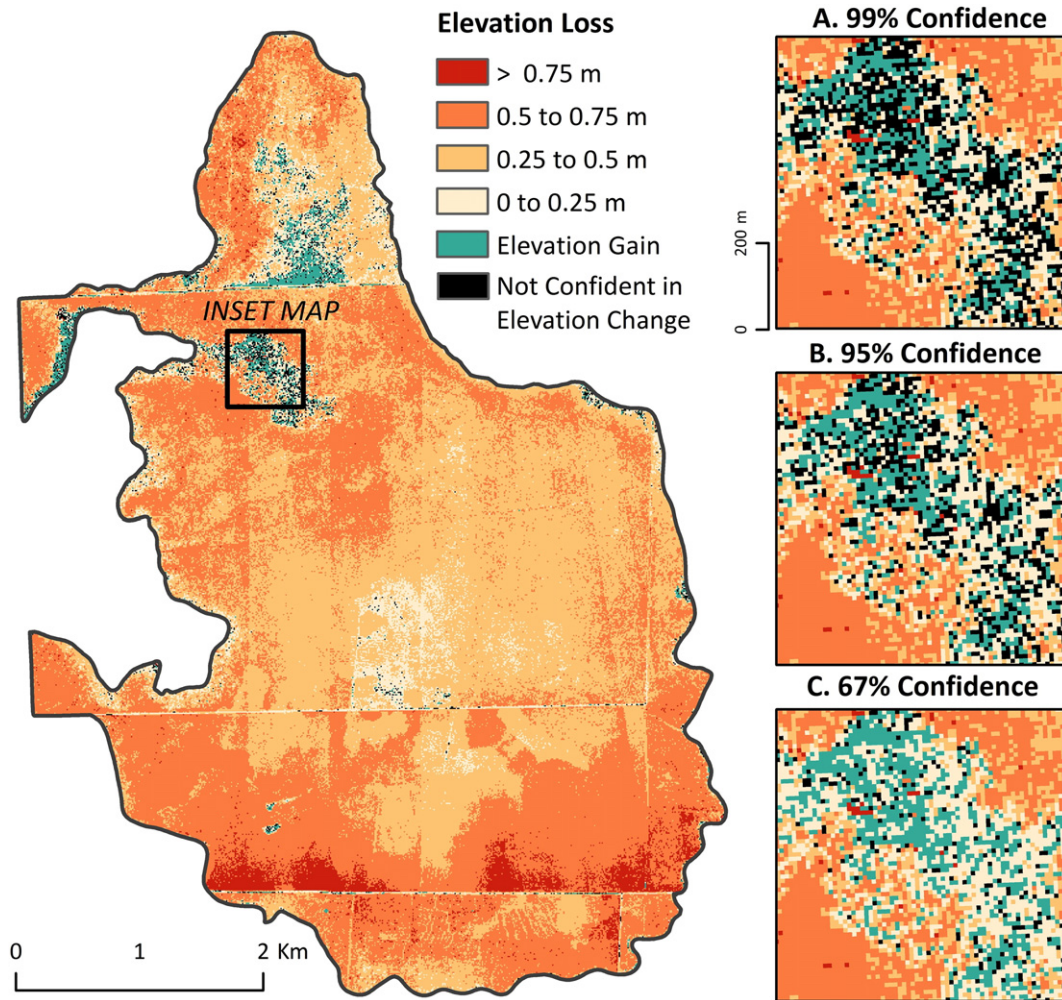


Fig. 5. The map at left depicts elevation change between 2010 and 2012; areas with no significant elevation change at the 95% confidence level are masked in black. The three maps to the right show elevation change at three confidence levels at finer resolution and with insignificant elevations masked in black at different confidence intervals: (A) 99%, (B) 95%, and (C) 67%.

buffer surrounding the fire scar, a 6 ± 37 cm elevation loss was detected. Given that the USGS MTBS data found no fire damage outside of the perimeter, it would be expected that little to no change in elevation would be found between 2010 and 2012, the years of LiDAR acquisition. The minor elevation loss outside the perimeter points to a possible bias in the LiDAR data itself.

A close look at Fig. 4 (right) shows two main areas of non-zero elevation change, rather than uniform elevation decline across the entire buffer area. The first, along the western edge of the perimeter, largely shows ground elevation loss between 0.25 and 0.50 m. This area is west of a drainage ditch and road that run north to south. Given that no fire occurred in the area, it was unclear to GDSNWR personnel what may have led to the change (F. Wurster, written communication, September 5, 2014).

The second area of interest is located in the southeast corner of Fig. 4 (right), just outside the burn scar. Here, elevation gain upwards of 0.50 m is estimated from LiDAR. It is also unclear how this elevation change may have occurred. One possibility is that differences in seasonality of the LiDAR acquisition may have led to elevation discrepancies. The 2010 LiDAR was acquired under leaf-off conditions in March, while 2012 LiDAR data were obtained during leaf-on conditions in August. This discrepancy in the Julian dates would have allowed for vegetation to accumulate during the growing seasons, potentially limiting the number of LiDAR returns from the ground surface. This may have led to a slight overestimate of ground elevation in 2012, resulting in the determination of elevation gain.

Although these two areas of change outside the perimeter are curious, they do not point to a systematic bias in the LiDAR data. Furthermore, vegetation conditions within the burned area are much different than those outside it. Any potential regrowth of vegetation within the burned area would likely bias the post-fire elevation measures upward. If vegetation had influenced the LiDAR returns, this would have influenced our estimates of elevation change conservatively. Thus, in conjunction with pre- and post-fire photos and MTBS data, the LiDAR data are likely to accurately reflect the surface elevations within Great Dismal Swamp.

In examining Fig. 6, we see that soil carbon loss varies spatially. The distinct horizontal and vertical lines in the maps represent the roads and ditches that traverse the refuge. This infrastructure acted as a fire-break and effectively isolated some tracts of land from significant fire damage. Other portions of the study site underwent minimal changes in soil elevation, which might suggest that only aboveground biomass was fire-affected in these areas, if at all. The most heavily affected areas were in the southern portion of the burn scar, much of which had burned previously in 2008. The depth of the burn, over a half-meter in these areas, has led to a longer period of standing water. Given this development, emergent vegetation has become common in the landscape (Fig. 2; bottom-right). As the next section will demonstrate, the magnitude of the Lateral West emissions was small compared to other peatland and non-peatland fires. Yet, the land that was affected was severely changed through loss of canopy, understory and soil. Given the changes in water table already witnessed in parts of the fire

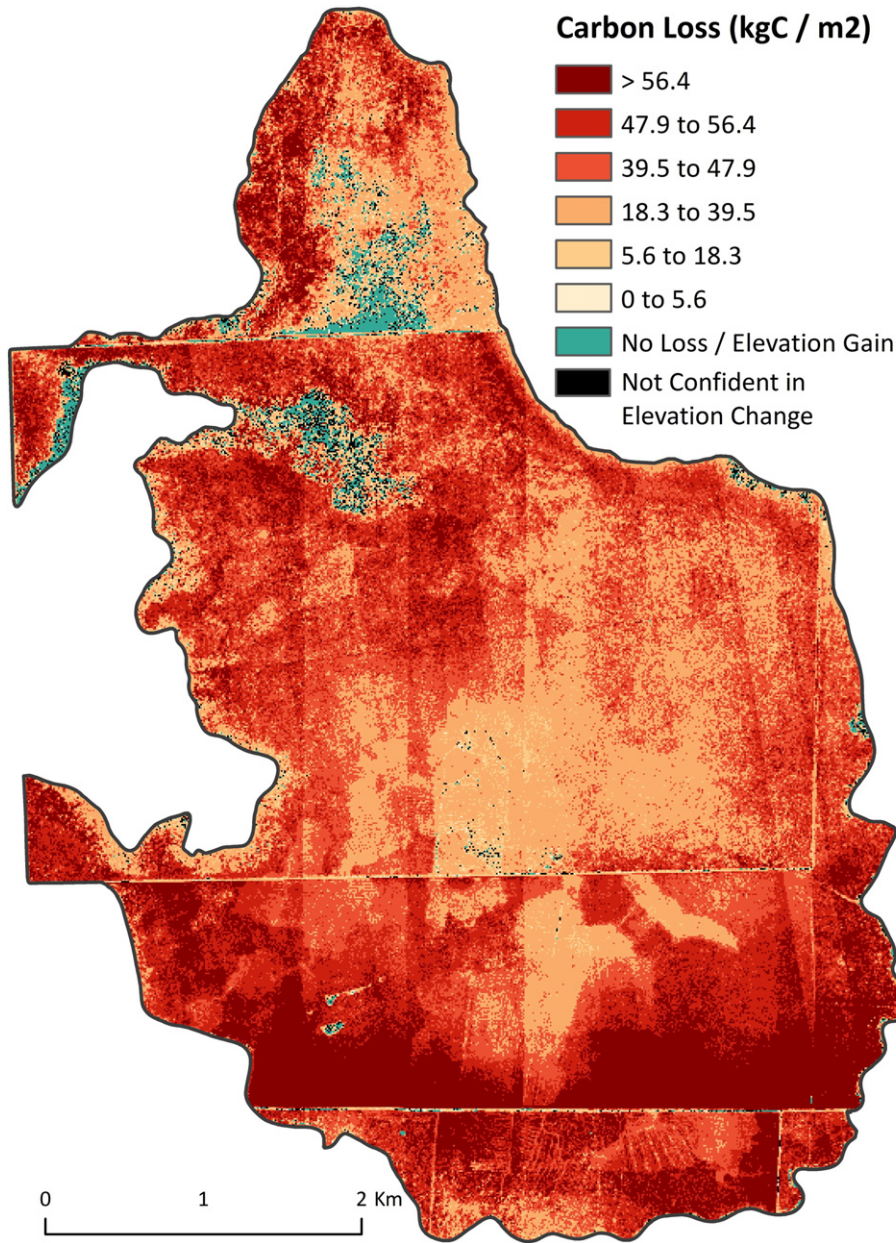


Fig. 6. Map of soil carbon loss (kg C/m²) classified into six quantiles.

scar, recovery is unlikely to involve pre-fire species that cannot adapt to the new environmental conditions.

4.3. Comparison to other studies of fire carbon emissions

The 2011 fire and the resulting carbon emissions estimates provided in this paper are compared to carbon loss values from other peatland fire studies in Table 3. GDSNWR total emissions were similar to estimates

from a North Carolina peat fire (Poulter et al., 2006). Although GDSNWR's 25 km² burned area was smaller than the 384 km² in the 1985 North Carolina fire, total carbon loss was similar in magnitude. As a result, carbon loss per unit-area at Great Dismal Swamp was considerably higher than in the Poulter et al. (2006) study. In the North Carolina study, soil carbon loss was estimated to be 0.31, 1.53, or 3.05 Tg C when assuming an average peat burn depth of 0.01, 0.05, or 0.10 m, respectively. This paper found that carbon loss from Lateral West was 1.1 Tg C, as estimated

Table 2

FOFEM greenhouse gas emissions (kg Carbon per m² burned) estimates for different combinations of burn severities (MTBS) and fuel loading models (FLM).

FLM	Description	% of total burned area	Carbon emissions by MTBS Class		
			Unburned to very-low	Low	Moderate
11	Light fine woody debris, Light to no duff	25%	0.035	0.045	0.056
21	Light logs, light duff	26%	0.063	0.077	0.090
63	Moderate duff, light to heavy logs, light litter	27%	0.128	0.157	0.192
101	Very heavy duff	22%	0.242	1.439	1.451

Table 3
Comparison of peatland fire carbon loss estimates.

Study	Location	Burned area (km ²)	C loss (Tg C)	C loss (kg C/m ²)
Page et al. (2002)	Indonesia (study area)	7300	~210	~28.8
Poulter et al. (2006)	NC, USA (0.1 m Est. burn)	384	3.05	7.57
Mack et al. (2011)	Alaska, USA	1039	2.1	2.02
This study (LiDAR)	GDSNWR, VA, USA	25	1.10	44.3
This study (model)	GDSNWR, VA, USA	25	0.06	2.32

from a LiDAR-based method. Bulk density used for the North Carolina peat (0.147 g/cm³) was similar to this study (0.16 g/cm³).

The 2007 peat fire on the North Slope of Alaska, USA, was also similar in magnitude to Lateral West with an estimated 2.1 Tg C burned (Mack et al., 2011). The fire burned over 1000 km², resulting in a unit-area carbon loss much lower than the GDSNWR fire.

Each of the peatland fires discussed above pale in comparison to the magnitude of the Indonesian peat fires studied by Page et al. (2002). These 1997 fires occurred during a dry El Nino year and burned 7300 of the 25,000 km² study area examined. Despite considerable differences in total carbon loss, unit-area loss in GDSNWR (44 kg C/m²) actually exceeds the 28.8 kg C/m² emissions estimated in the Central Kalimantan, Indonesia study area. Part of this discrepancy may be due to Page et al. (2002) applying a lower bulk density value (0.10 g/cm³) than this study (0.16 g/cm³).

Together these comparisons suggest that either (1) previous studies underestimated carbon loss from peatland fires, or (2) the severity of the soil carbon loss from the 2011 fire in Great Dismal was unlike many previously studied peatland fires. If the former explanation is true, using multi-temporal LiDAR would likely provide the most precise understanding of elevation change and carbon loss following peat fire. Assumptions about elevation change, derived from burned-unburned analogs or maximum potential burn depths, do not provide the level of certainty that LiDAR remote sensing does. Although LiDAR can be cost-prohibitive and impractical in certain situations, the results for the Lateral West fire demonstrate the technology's capability.

Table 4 compares LiDAR-based and FOFEM-modeled carbon loss from the Lateral West incident with emissions modeled by French et al. (2011) using FOFEM 5.7 of five other wildland fire occurrences in North America. These fires range from the chaparral of the southwestern USA to the boreal conifer forests of Alaska and Canada. Unit-area carbon loss estimates for the French et al. fires were small relative to the LiDAR-based estimate of the Lateral West fire (44.3 kg C/m²). The sources of carbon in the fires studied by French et al. largely stemmed from aboveground biomass, woody debris, and surface fuels. Meanwhile, the high unit-area emissions from the Lateral West fire resulted from burning of belowground fuels, namely the organic, carbon-rich peat soils of GDSNWR. Several of the fires in Table 4, such as the Biscuit and Boundary events, consumed over 1000 km² of land. Despite the small magnitude of total carbon loss compared to these other wildfires, the 2011 Lateral West fire resulted in substantially more emissions per unit-area.

Table 4
Comparison of Lateral West to French et al. (2011) FOFEM-modeled emissions of other North American wildland fires under dry fuel conditions.

Fire	Year	Location	Description	Burned area (km ²)	Carbon loss (Tg C)	Carbon loss (kg C/m ²)
Lateral West (This study – LiDAR)	2011	GDSNWR, VA, USA	Forested wetlands	25	1.10	44.3
Lateral West (This study – FOFEM)	2011	GDSNWR, VA, USA	Forested wetlands	25	0.06	2.3
Boundary	2004	AK, USA	Black Spruce/Feather Moss Forest	2172	12.0	5.5
Montreal Lake	2003	Saskatchewan, Canada	Mixed Conifer and Broadleaf Forest	217	1.3	5.9
Biscuit	2002	OR, USA	Conifer Forests	2000	3.7	1.8
Cedar, Paradise, and Mine-Otay	2003	CA, USA	Chaparral Shrublands	1438	1.5	1.0
Witch, Harris, and Poomacha	2007	CA, USA	Chaparral Shrublands	1200	1.2	1.1

4.4. LiDAR vertical accuracy error

Unlike previous LiDAR-based fire studies, this effort used both pre- and post-fire elevation data to precisely assess the amount of below-ground carbon that was consumed and emitted to the atmosphere. To ensure that this remote sensing method would be appropriate for assessing carbon loss from other fires, it was necessary to understand whether LiDAR vertical accuracy error might contribute to uncertainty in our emissions estimates. Our results demonstrated that LiDAR elevation error was equivalent to just 0.008% of the total 1.10 Tg C loss.

The LiDAR error analysis also helped to identify areas within the fire perimeter where the elevation change might be suspect (Fig. 5). For these pixels, elevation change was much less than the 9 or 7 cm LiDAR RMSEs, so we did not have enough confidence to classify them as either elevation loss or gain. Depending on the level of confidence applied, between 0.16 and 0.89% of pixels within the Lateral West might adversely affect carbon loss calculations. However, given the magnitude of the 2011 fire, these effects are small.

In low severity fires, when the average soil loss is equal to the LiDAR elevation errors, propagating the uncertainty may prove important. For example, take a point with a pre-fire elevation of 19 cm that drops to 12 cm post-fire, and 7 cm RMSEs for the LiDAR datasets from which these numbers came. Simulating normal distributions for these two elevations based on the 7 cm average error demonstrates that 24% of the time the post-fire elevations are actually greater than the pre-fire elevations. There is a large probability that what appears to be a 7 cm soil loss may actually be a soil gain when factoring in the LiDAR vertical accuracy error. Thus, it becomes difficult to discern whether or not this elevation change is real or an artifact of sensor error.

The error analysis is less important under a severe peat fire when the average soil loss is much greater than the LiDAR elevation error. Take an area with pre- and post-fire elevations of 33 and 12 cm, respectively. In this situation, the 21 cm elevation drop is three times the 7 cm LiDAR error, and the likelihood that the soil loss is actually a soil gain is just 1.7%. In this instance, there is less uncertainty about the direction of elevation change.

Fig. 7 shows the likelihood of drawing a false conclusion about elevation change given how large that change is relative to LiDAR error. If, as in the previous example, the ratio of elevation change to LiDAR error is 3 (x-axis), then there is a 1.7% chance of assuming an elevation loss when there is actually a gain (y-axis). With increasing values of x, when elevation change becomes much larger than LiDAR error, there becomes a

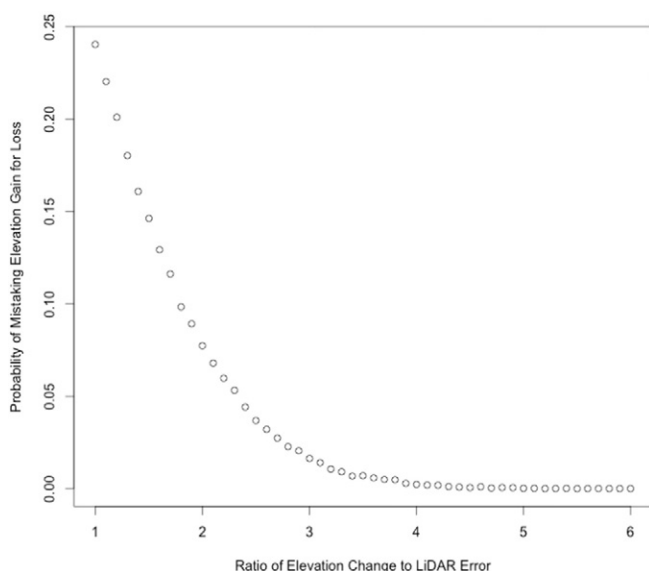


Fig. 7. Probability of misidentifying elevation gain as loss (or loss as gain) given the ratio of elevation change to LiDAR error. In high-severity peat fires, elevation change would be much larger than LiDAR error, so there is little chance of misjudging the direction of soil surface change. By contrast, low-severity fires are more prone to uncertainty brought on by vertical accuracy error.

very small chance of making an erroneous conclusion about how fire has affected the soil surface. Fig. 7 is a helpful guide for determining when to analyze the influence of vertical accuracy error on LiDAR-based elevation change estimates. We agree with past studies (Jaw, 2001; Jones et al., 2013) that uncertainty be quantified when average elevation change is less than three times the LiDAR vertical error.

Our study isolated the effects of LiDAR point elevation errors on carbon loss without addressing other potential sources of uncertainty. Additional errors related to DEM creation or LiDAR ground filtering, for example, could complicate efforts to accurately estimate fire emissions. Other studies have tackled these matters though (Bater & Coops, 2009; Sithole & Vosselman, 2004), and this work simply adds an additional perspective on the use of LiDAR for understanding fire carbon emissions.

5. Conclusion

Previous studies of peatland carbon loss due to fire (Page et al., 2002; Poulter et al., 2006) were constrained by unideal methods for determining changes in soil elevation. We overcome this by obtaining LiDAR elevation data from before and after the fire at Great Dismal Swamp. We found that although total emissions from the 2011 fire were much less than those from the 1997 Indonesian peat fires, the carbon loss on a per unit-area basis was greater at GDSNWR, where a long history of draining has extensively altered the site's hydrology. This has resulted in drier conditions in the GDSNWR peatlands and possibly increased their exposure to wildfire.

The large unit-area carbon estimate at GDSNWR suggests that classifying fires based on the total area burned might not be appropriate for describing the extent of ecological disturbance in peat environments. Although the Lateral West fire burned just 25 km², the amount of soil lost was large (~11.7 million m³). Thus, when data permit, a soil volume statistic might provide a better understanding of fire severity than burned area. This is particularly true for regions with deep, carbon-rich organic soil like Siberia and the tropical peat domes of Indonesia (Langmann & Heil, 2004; Sheng et al., 2004). Soil carbon loss in these regions can dwarf emissions from aboveground biomass, and total peat depths often exceed one meter.

When possible, the pre- and post-fire LiDAR method used in this study would likely improve fire emissions estimates in peatland

ecosystems. When utilizing this remote sensing method, we find that LiDAR vertical accuracy error has the potential to adversely affect estimates of soil elevation and carbon loss. Propagating the LiDAR error in these estimates is important for confidently identifying soil loss versus gain and precisely quantifying soil carbon change, particularly under low-severity fires. For the Lateral West fire and others of similar magnitude, LiDAR vertical accuracy error has a more limited effect on these calculations.

The ecosystems within GDSNWR have historically been subject to fire disturbance. Fire is considered an important process for resetting biomass and facilitating species establishment in the pre-settlement era (Bailey, Mickler, & Frost, 2007; Frost, 1989, 1995). However, more than 200 years of hydrologic alteration and the lowering of the water table have made the GDSNWR especially fire prone. Using water control structures along drainage ditches, the U.S. Fish and Wildlife Service is attempting to re-wet the organic soils of the refuge to provide conditions more appropriate to native plant species. Although restoration of the site to pre-settlement vegetation conditions is unlikely given environmental changes, more control over the flow of water could limit burn severity in future fires, protect the accumulated peat and help to sequester soil carbon going forward. Since peatlands account for a disproportionately large share of global soil carbon, limiting severe fires and re-wetting drained peatlands like Great Dismal Swamp might be important strategies for mitigating future carbon emissions (Lal, 2004).

Acknowledgments

We are grateful to the U.S. Geological Survey, Climate and Land Use Mission Area Land Change Science and Land Remote Sensing Programs for providing funding to support this research. We also thank the U.S. Fish and Wildlife Service for their support and participation in this project. The USDA Natural Resources Conservation Service's Kellogg Soil Survey Lab in Lincoln, NE, graciously analyzed samples and provided guidance on sample collection. NRCS scientists Greg Hammer and Rachel Stull helped guide the soil sampling protocol in Virginia while NRCS interns Elizabeth Ruiz and Aaron Hayes assisted with sample collection. Rich Ferguson and Steve Monteith coordinated soil analyses at the Kellogg Soil Survey Lab. Two anonymous reviewers, Jay Diffendorfer, Jason Stoker and Janet Slate provided insightful comments on this manuscript and their comments helped to improve its completeness and clarity. Any use of trade, product, or firm names is for descriptive purposes only and does not imply endorsement by the U.S. Government.

References

- Bailey, A. D., Mickler, R., & Frost, C. C. (2007 March). Presettlement fire regime and vegetation mapping in Southeastern Coastal Plain forest ecosystems. In B. W. Butler, & W. Cook (Eds.), *The fire environment—innovations, management, and policy*. USDA Forest Service Proceedings, U.S. Department of Agriculture, Forest Service (pp. 26–30) (Destin, FL) http://www.fs.fed.us/rm/pubs/rmrs_p046/rmrs_p046_275_286.pdf.
- Ballhorn, U., Siegert, F., Mason, M., & Limin, S. (2009). Derivation of burn scar depths and estimation of carbon emissions with LiDAR in Indonesian peatlands. *Proceedings of the National Academy of Sciences*, 106(50), 21213–21218. <http://dx.doi.org/10.1073/pnas.0906457106>.
- Bater, C. W., & Coops, N. S. (2009). Evaluating error associated with LiDAR-derived DEM interpolation. *Computers and Geosciences*, 35(2), 289–300.
- Batjes, N. H. (1996). Total carbon and nitrogen in the soils of the world. *European Journal of Soil Science*, 47(2), 151–163. <http://dx.doi.org/10.1111/j.1365-2389.1996.tb01386.x>.
- Clymo, R. S. (1984). The limits to peat bog growth. *Philosophical Transactions of the Royal Society of London B Biological Sciences*, 303(1117), 605–654. <http://dx.doi.org/10.1098/rstb.1984.0002>.
- Day, F. P., Jr. (1982). Litter decomposition rates in the seasonally flooded great dismal swamp. *Ecology*, 63(3), 670–678. <http://dx.doi.org/10.2307/1936787>.
- Eidenshink, J., Schwind, B., Brewer, K., Zhu, Z. L., Quayle, B., & Howard, S. (2007). *Project for monitoring trends in burn severity*. *Fire Ecology*.
- French, N. H. F., de Groot, W. J., Jenkins, L. K., Rogers, B. M., Alvarado, E., Amiro, B., ... Turetsky, M. (2011). Model comparisons for estimating carbon emissions from North American wildland fire. *Journal of Geophysical Research: Biogeosciences*, 116(G4), G00K05. <http://dx.doi.org/10.1029/2010JG001469>.
- Frost, C. C. (1989). *History and status of remnant pocosin, canebrake, and white cedar wetlands in Virginia*. Report to Virginia Natural Heritage Program.

- Frost, C. C. (1995). Presettlement fire regimes in southeastern marches, peatlands, and swamps. In S. I. Cerulean, & R. T. Engstrom (Eds.), *Fire in wetlands: A management perspective. Proceedings of the Tall Timbers Fire Ecology Conference, 19*. Tallahassee: Tall Timbers Research Station.
- Gorham, E. (1991). Northern peatlands: Role in the carbon cycle and probable responses to climatic warming. *Ecological Applications*, 1(2), 182–195. <http://dx.doi.org/10.2307/1941811>.
- Hawbaker, T., & Zhu, Z. (2012). Baseline wildland fires and emissions for the Western United States. In Z. Zhu, & B. Reed (Eds.), *Baseline and projected future carbon storage and greenhouse-gas fluxes in ecosystems of the Western United States. U.S. Geological Survey Professional Paper, 1797*. (pp. 192) (Also available at <http://pubs.usgs.gov/pp/1797/>).
- Hodgson, M. E., & Bresnahan, P. (2004). Accuracy of airborne lidar-derived elevation. *Photogrammetric Engineering and Remote Sensing*, 70(3), 331–339. <http://dx.doi.org/10.14358/PERS.70.3.331>.
- Jaw, J. (2001). Statistics-based fusion of terrain data sets and change detection. *proceedings, 22nd Asian conference on remote sensing, Singapore, November 5–9, 2001*. Singapore: Centre for Remote Imaging, Sensing and Processing, National University of Singapore (6 pp.).
- Jones, B. M., Stoker, J. M., Gibbs, A. E., Grosse, G., Romanovsky, V. E., Douglas, T. A., ... Richmond, B. M. (2013). Quantifying landscape change in an Arctic coastal lowland using repeat airborne LiDAR. *Environmental Research Letters*, 8(4), 1–10.
- Lal, R. (2004). Soil carbon sequestration to mitigate climate change. *Geoderma*, 123(1–2), 1–22. <http://dx.doi.org/10.1016/j.geoderma.2004.01.032>.
- Langmann, B., & Heil, A. (2004). Release and dispersion of vegetation and peat fire emissions in the atmosphere over Indonesia 1997/1998. *Atmospheric Chemistry and Physics*, 4(8), 2145–2160. <http://dx.doi.org/10.5194/acp-4-2145-2004>.
- Levy, G. F. (1991). The vegetation of the great dismal swamp: A review and an overview. *Virginia Journal of Science*, 42(4), 411–417.
- Lily, J. P. (1981 Jan 3–4). A history of swamp land development in North Carolina. In C. L. Richardson (Ed.), *Proceedings of Pocosins: a Conference on Alternative Uses of the Coastal Plain Freshwater Wetlands of North Carolina* (pp. 20–39). Beaufort, NC, U.S.A.: Duke University Marine Laboratory.
- Lutes, D. (2012). *FOFEM 6.0 user guide*. Fort Collins, CO: USDA Forest Service, Rocky Mountain Research Station (Available at http://www.firelab.org/ScienceApps_Files/downloads/FOFEM/FOFEM6_Help.pdf [Verified 7 May 2013]).
- Lutes, D. C., Keane, R. E., & Caratti, J. F. (2009). A surface fuel classification for estimating fire effects. *International Journal of Wildland Fire*, 18(7), 802–814.
- Mack, M. C., Bret-Harte, M. S., Hollingsworth, T. N., Jandt, R. R., Schuur, E. A. G., Shaver, G. R., & Verbyla, D. L. (2011). Carbon loss from an unprecedented Arctic tundra wildfire. *Nature*, 475(7357), 489–492.
- Mälson, K., Bäckéus, I., & Rydin, H. (2007). Long-term effects of drainage and initial effects of hydrological restoration on rich fen vegetation. *Applied Vegetation Science*, 11(1), 99–106. <http://dx.doi.org/10.3170/2007-7-18329>.
- Minkinen, K., & Laine, J. (1998). Effect of forest drainage on the peat bulk density of pine mires in Finland. *Canadian Journal of Forest Research*, 28(2), 178–186. <http://dx.doi.org/10.1139/x97-206>.
- Mitsch, W. J., Gosselink, J. G., Anderson, C. J., & Zhang, L. (2009). *Wetland ecosystems*. Hoboken, NJ, U.S.A.: John Wiley and sons.
- Page, S. E., Rieley, J. O., & Banks, C. J. (2011). Global and regional importance of the tropical peatland carbon pool. *Global Change Biology*, 17(2), 798–818. <http://dx.doi.org/10.1111/j.1365-2486.2010.02279.x>.
- Page, S. E., Siegert, F., Rieley, J. O., Boehm, H. -D. V., Jaya, A., & Limin, S. (2002). The amount of carbon released from peat and forest fires in Indonesia during 1997. *Nature*, 420(6911), 61–65. <http://dx.doi.org/10.1038/nature01131>.
- Peterson, T. C., & Vose, R. S. (1997). An overview of the global historical climatology network temperature database. *Bulletin of the American Meteorological Society*, 78(12), 2837–2849.
- Poulter, B., Christensen, N. L., & Halpin, P. N. (2006). Carbon emissions from a temperate peat fire and its relevance to interannual variability of trace atmospheric greenhouse gases. *Journal of Geophysical Research: Atmospheres*, 111(D6), D06301 <http://dx.doi.org/10.1029/2005JD006455>.
- Pronger, J., Schipper, L. A., Hill, R. B., Campbell, D. I., & McLeod, M. (2014). Subsidence rates of drained agricultural peatlands in New Zealand and the relationship with time since drainage. *Journal of Environmental Quality*, 43(4), 1442. <http://dx.doi.org/10.2134/jeq2013.12.0505>.
- Reardon, J., Curcio, G., & Bartlette, R. (2009). Soil moisture dynamics and smoldering combustion limits of pocosin soils in North Carolina, U.S.A. *International Journal of Wildland Fire*, 18, 326–335.
- Reinhardt, E. D., Keane, R. E., & Brown, J. K. (1997). *First Order Fire Effects Model: FOFEM 4.0, user's guide Retrieved from http://www.treesearch.fs.fed.us/pubs/25257*
- Richardson, C. J. (1983). Pocosins: Vanishing wastelands or valuable wetlands? *Bioscience*, 33(1), 626–633.
- Schoeneberger, P. J., Wysocki, D. A., Benham, E. C., & Broderson, W. D. (Eds.). (2002). *Field book for describing and sampling soils, version 2.0*. Lincoln, NE: Natural Resources Conservation Service, National Soil Survey Center.
- Sheng, Y., Smith, L. C., MacDonald, G. M., Kremenetski, K. V., Frey, K. E., Velichko, A. A., ... Dubinin, P. (2004). A high-resolution GIS-based inventory of the west siberian peat carbon pool. *Global Biogeochemical Cycles*, 18(3), GB3004. <http://dx.doi.org/10.1029/2003GB002190>.
- Sithole, G., & Vosselman, G. (2004). Experimental comparison of filter algorithms for bare-earth extraction from airborne laser scanning point clouds. *ISPRS Journal of Photogrammetry and Remote Sensing*, 59(1–2), 85–101.
- Talbot, J., Richard, P. J. H., Roulet, N. T., & Booth, R. K. (2010). Assessing long-term hydrological and ecological responses to drainage in a raised bog using paleoecology and a hydrosequence. *Journal of Vegetation Science*, 21(1), 143–156. <http://dx.doi.org/10.1111/j.1654-1103.2009.01128.x>.
- Tarnocai, C., Canadell, J. G., Schuur, E. A. G., Kuhry, P., Mazhitova, G., & Zimov, S. (2009). Soil organic carbon pools in the northern circumpolar permafrost region. *Global Biogeochemical Cycles*, 23(2), GB2023. <http://dx.doi.org/10.1029/2008GB003327>.
- Terrasolid (2005). *TerraScan User's Guide*.
- Thompson, G. S., Belcher, R. T., & Atkinson, R. B. (2000). Soil biogeochemistry in Virginia and North Carolina Atlantic white cedar swamps. In R. Atkinson, R. Belcher, D. Brown, & J. Perry (Eds.), *Atlantic White Cedar Restoration Ecology and Management. Paper presented at Christopher Newport University, Newport News, Virginia, 31 May–2 June 2000* (pp. 113–124).
- Turetsky, M. R., Donahue, W. F., & Benscotter, B. W. (2011). Experimental drying intensifies burning and carbon losses in a northern peatland. *Nature Communications*, 2, 514. <http://dx.doi.org/10.1038/ncomms1523>.
- Turunen, J., Tomppo, E., Tolonen, K., & Reinikainen, A. (2002). Estimating carbon accumulation rates of undrained mires in Finland—application to boreal and subarctic regions. *The Holocene*, 12(1), 69–80. <http://dx.doi.org/10.1191/0959683602hl522rp>.
- Yu, Z., Loisel, J., Brosseau, D. P., Beilman, D. W., & Hunt, S. J. (2010). Global peatland dynamics since the Last Glacial Maximum. *Geophysical Research Letters*, 37(13), L13402. <http://dx.doi.org/10.1029/2010GL043584>.